Supplementary Information

Highly Efficient Hydrogen Sensors Based on Pd Nanoparticles Supported on Boron Nitride Coated ZnO Nanowires

Matthieu Weber,[‡,†] Jin-Young Kim,[§,†] Jae-Hyoung Lee,[§] Jae-Hun Kim,[§] Igor Iatsunskyi,[×] Emerson Coy,[×] Philippe Miele,[‡,α] Mikhael Bechelany,[‡,] and Sang Sub Kim[§,*]*

[‡] Institut Européen des Membranes, IEM – UMR 5635, ENSCM, CNRS, University of Montpellier, Place Eugène Bataillon, 34095 Montpellier cedex 5, France.

[§] Department of Materials Science and Engineering, Inha University, Incheon 22212, Republic of Korea.

[α] Institut Universitaire de France, 1 rue Descartes, 75231 Paris, France.

[×] NanoBioMedical Centre, Adam Mickiewicz University in Poznan, 61-614, Umultowska str. 85 Poznan, Poland.

Table S1. Comparison between the ZnO-based hydrogen gas sensors in present study with those reported in the literature.

Sensor	H_2 conc. (ppm)	T (°C)	Response	Ref.
Pd/BN/ZnO	50	200	12.28[a]	This work
Porous ZnO nanotubes	5000	200	8[a]	[1]
ZnO nanorods	100 ppm	340	5[a]	[2]
Mg doped ZnO thin films	5000	300	50[a]	[3]
WO_3-ZnO nanowire	2000	200	12.6[a]	[4]
Al doped ZnO thin film	1000	300	1.7[a]	[5]
Nanopillar ZnO	2500	350	30[a]	[6]
ZnO-0.5NiO	10	200	0.6[b]	[7]
Co-doped ZnO	50	150	2.3[a]	[8]
ZnO-SnO_2	10000	150	0.94[b]	[9]
ZnO NWs	1500	250	0.9[b]	[10]

a: (R_a/R_g), b: $([R_a-R_g]/R_a)$

(1) Choi, K.S. and Chang, S.P., 2018. Effect of structure morphologies on hydrogen gas sensing by ZnO nanotubes. *Materials Letters*, *230*, pp.48-52.

(2) Sun, Z.P., Liu, L., Zhang, L. and Jia, D.Z., 2006. Rapid synthesis of ZnO nano-rods by one-step, room-temperature, solid-state reaction and their gas-sensing properties. *Nanotechnology*, *17*(9), p.2266.

(3) Liu, Y., Hang, T., Xie, Y., Bao, Z., Song, J., Zhang, H. and Xie, E., 2011. Effect of Mg doping on the hydrogen-sensing characteristics of ZnO thin films. *Sensors and Actuators B: Chemical*, *160*(1), pp.266-270.

(4) Park, S., 2019. Enhancement of hydrogen sensing response of ZnO nanowires for the decoration of WO3 nanoparticles. *Materials Letters*, *234*, pp.315-318.

(5) M.T. Hosseinnejad, M. Ghoranneviss, M.R.Hantehzadeh, E. Darabi, J. Mater. Sci., 27 (2016), pp. 11308-11318.

(6) Bie, L.J., Yan, X.N., Yin, J., Duan, Y.Q. and Yuan, Z.H., 2007. Nanopillar ZnO gas sensor for hydrogen and ethanol. *Sensors and Actuators B: Chemical*, *126*(2), pp.604-608.

(7) Lee, J.H., Kim, J.Y., Mirzaei, A., Kim, H. and Kim, S., 2018. Significant enhancement of hydrogen-sensing properties of ZnO nanofibers through NiO loading. *Nanomaterials*, *8*(11), p.902.

(8) Moosavi, F., Bahrololoom, M.E., Kamjou, R., Mirzaei, A., Leonardi, S.G. and Neri, G., 2018. Hydrogen Sensing Properties of Co-Doped ZnO Nanoparticles. *Chemosensors*, *6*(4), p.61.

(9) Mondal, B., Basumatari, B., Das, J., Roychaudhury, C., Saha, H. and Mukherjee, N., 2014. ZnO–SnO2 based composite type gas sensor for selective hydrogen sensing. *Sensors and Actuators B: Chemical*, *194*, pp.389-396.

(10) Qurashi, A., Tabet, N., Faiz, M. and Yamzaki, T., 2009. Ultra-fast microwave synthesis of ZnO nanowires and their dynamic response toward hydrogen gas. *Nanoscale research letters*, *4*(8), p.948.

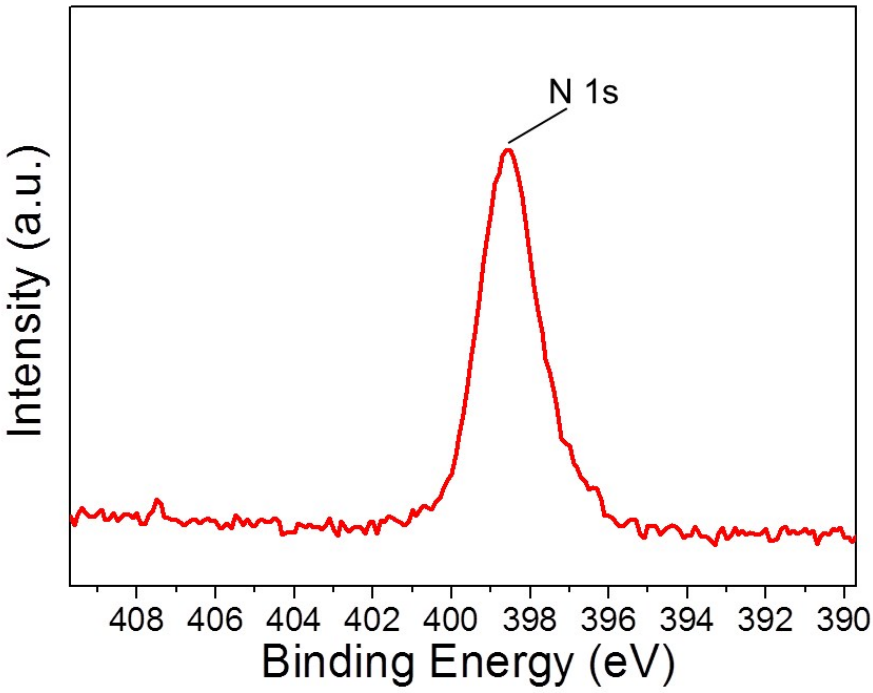

Figure S1. N1s XPS core-level region.

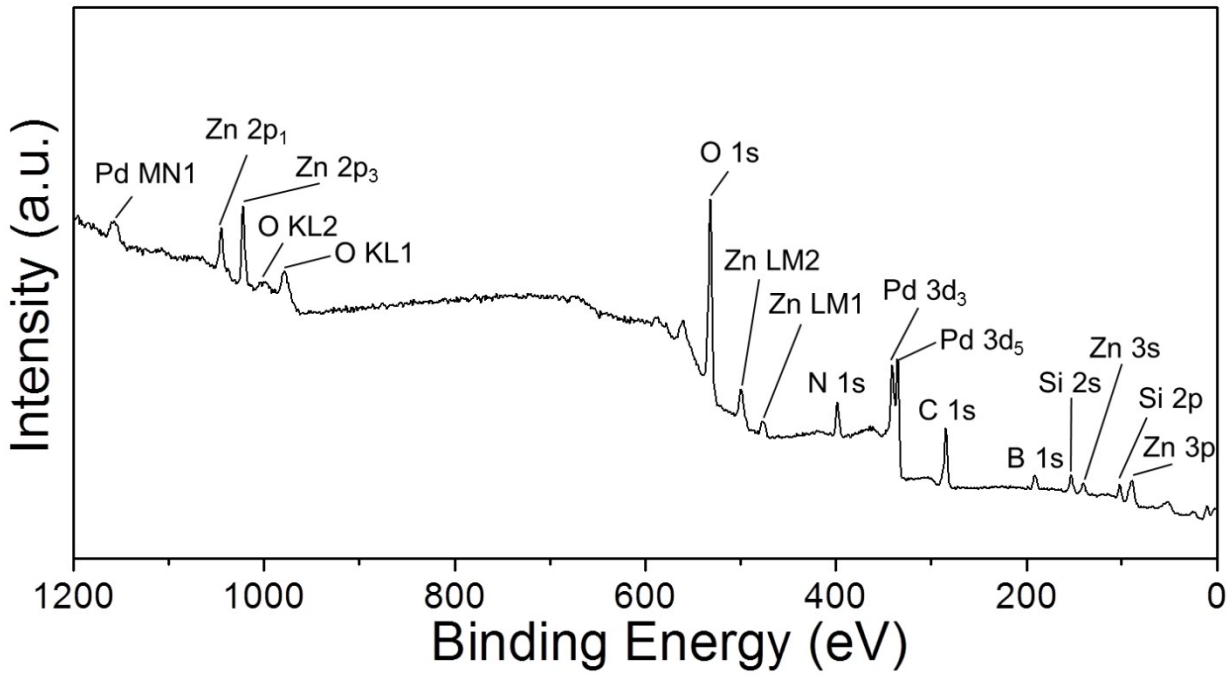

Figure S2. XPS overall scan of Pd/BN/ZnO sensor.

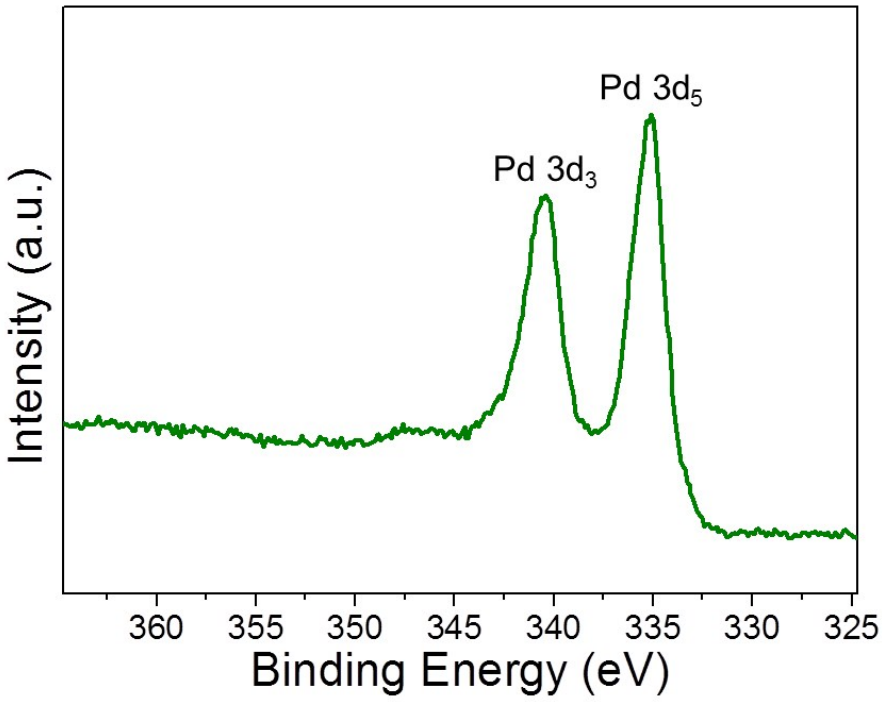

Figure S3. XPS P_{3d} core-level region.

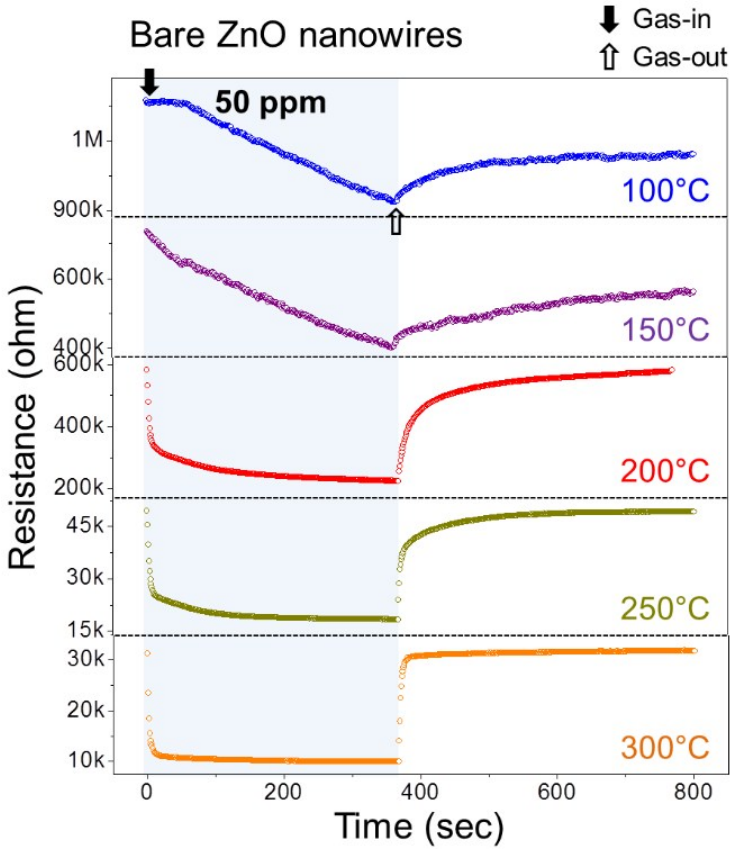

Figure S4. Dynamic resistance curves of bare ZnO NWs towards 50 ppm H_2 gas at different temperatures.

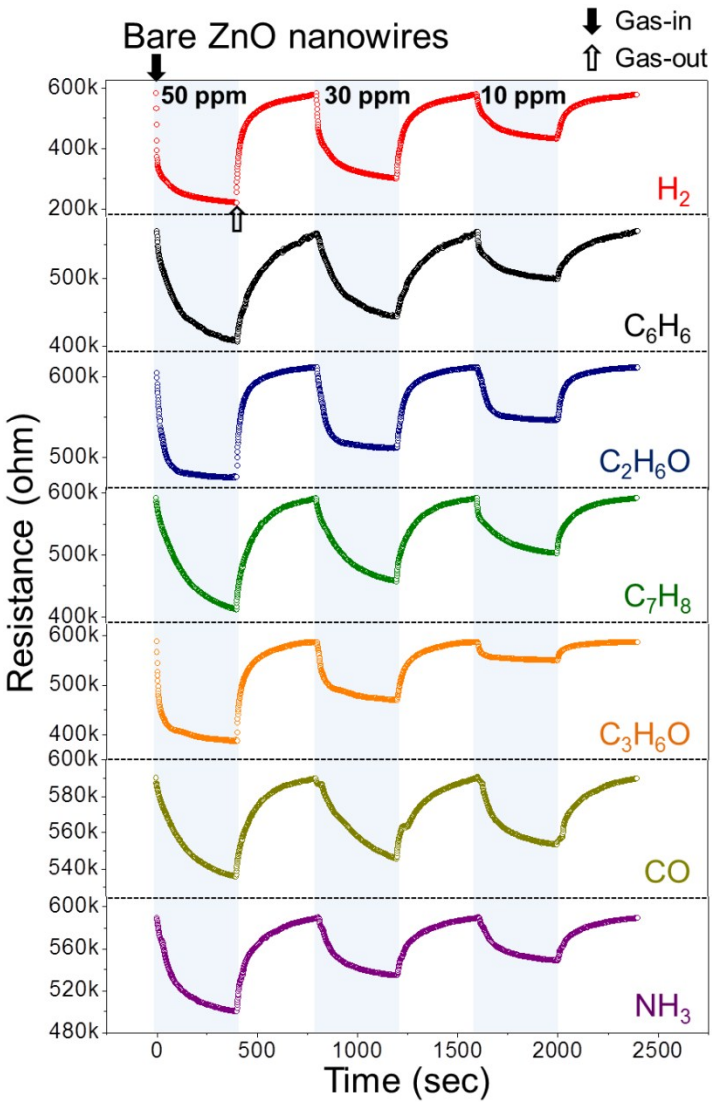

Figure S5. Dynamic resistance curves of bare ZnO NWs towards 10, 30 and 50 ppm of different gases at optimal sensing temperature.

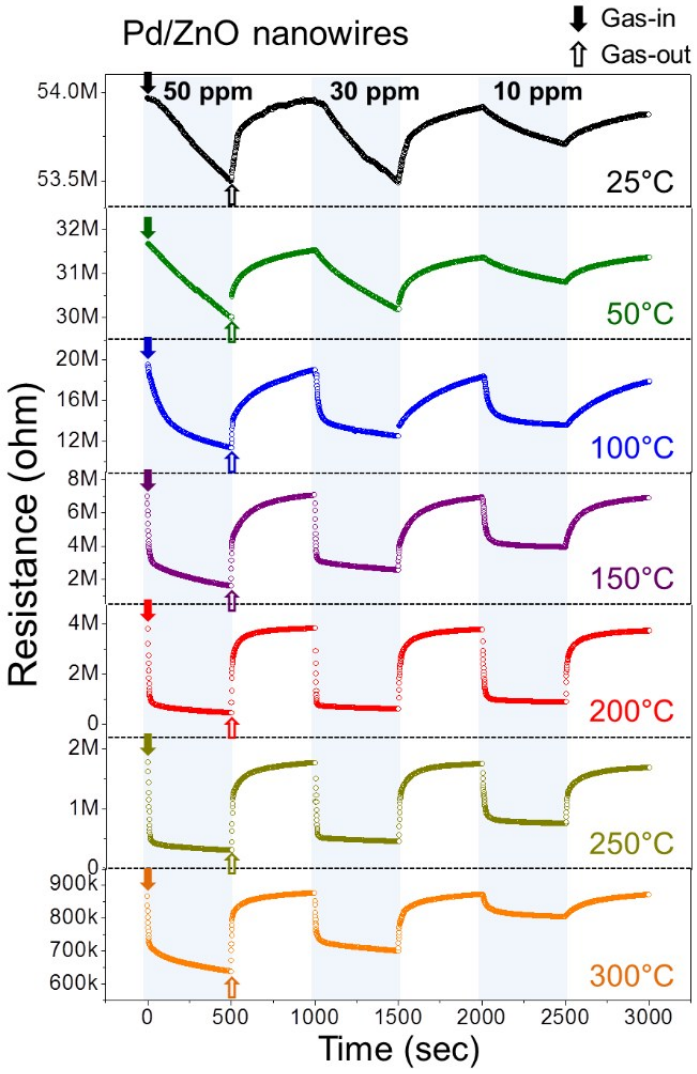

Figure S6. Dynamic resistance curves of Pd/ZnO NWs towards 10, 30 and 50 ppm H_2 gas at different temperatures.

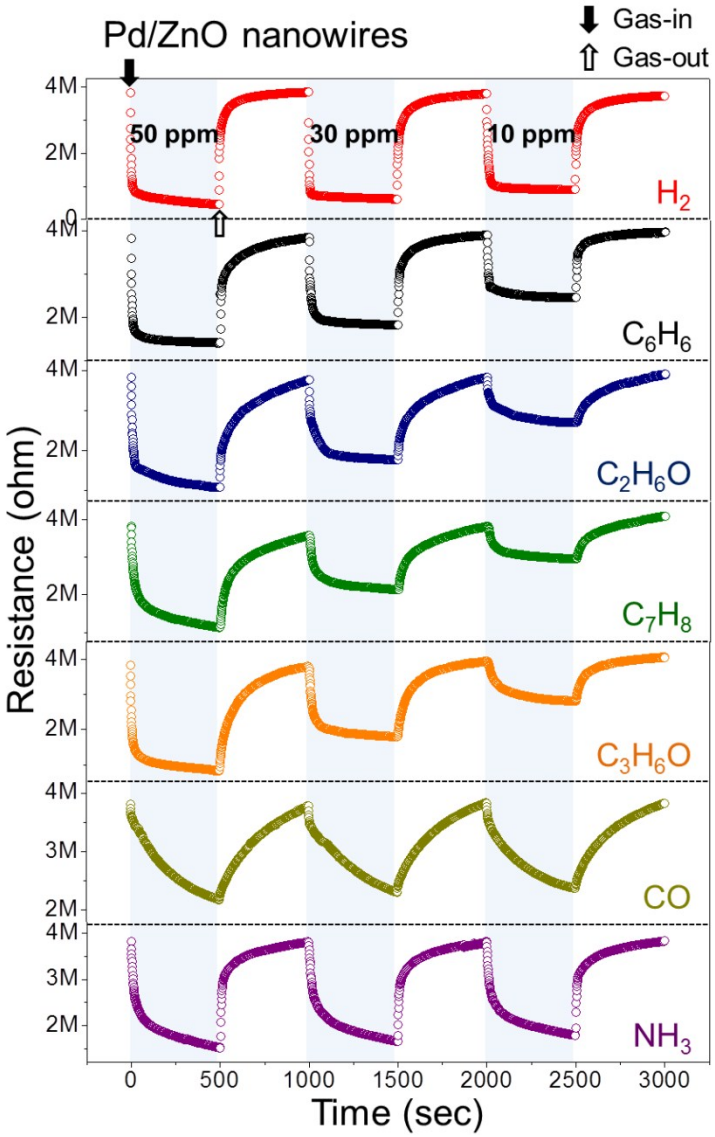

Figure S7. Dynamic resistance curves of Pd/ZnO NWs towards 10, 30 and 50 ppm different gases at 200°C.

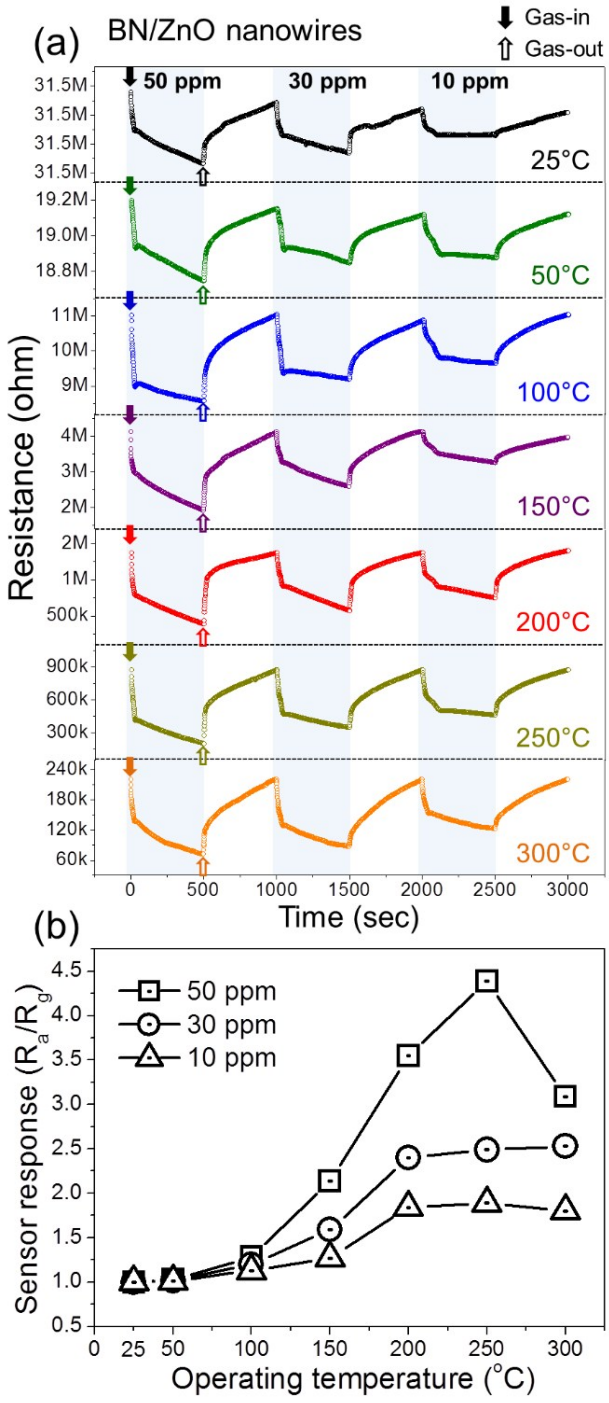

Figure S8. (a) Dynamic resistance curves of BN/ZnO NWs towards 10, 30 and 50 ppm H_2 gas at different temperatures. (b) Response versus operating temperature for different concentrations of H_2 gas.

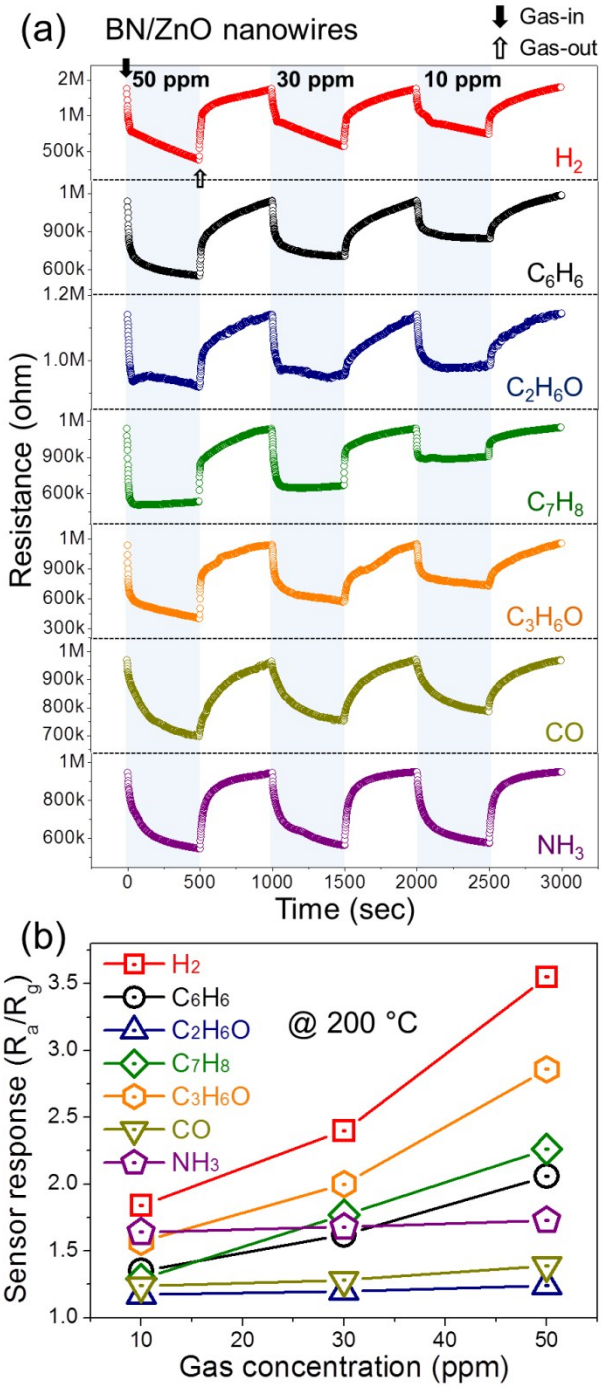

Figure S9. (a) Dynamic resistance curves of BN/ZnO NWs towards 10, 30 and 50 ppm different gases at 200°C. (b) Corresponding calibration curve.

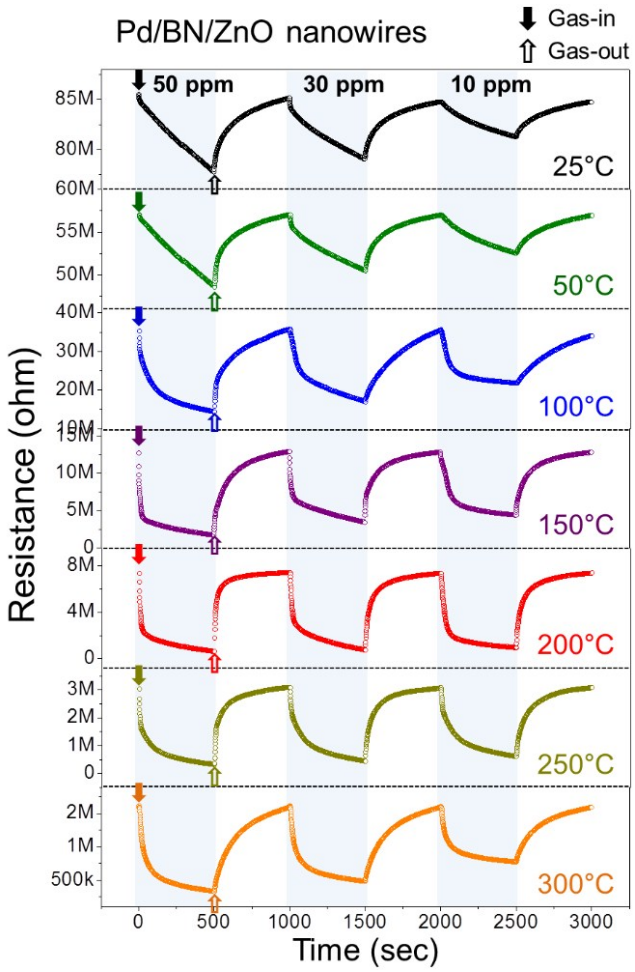

Figure S10. Dynamic resistance curves of Pd/BN/ZnO NWs towards 10, 30 and 50 ppm H_2 gas at different temperatures.

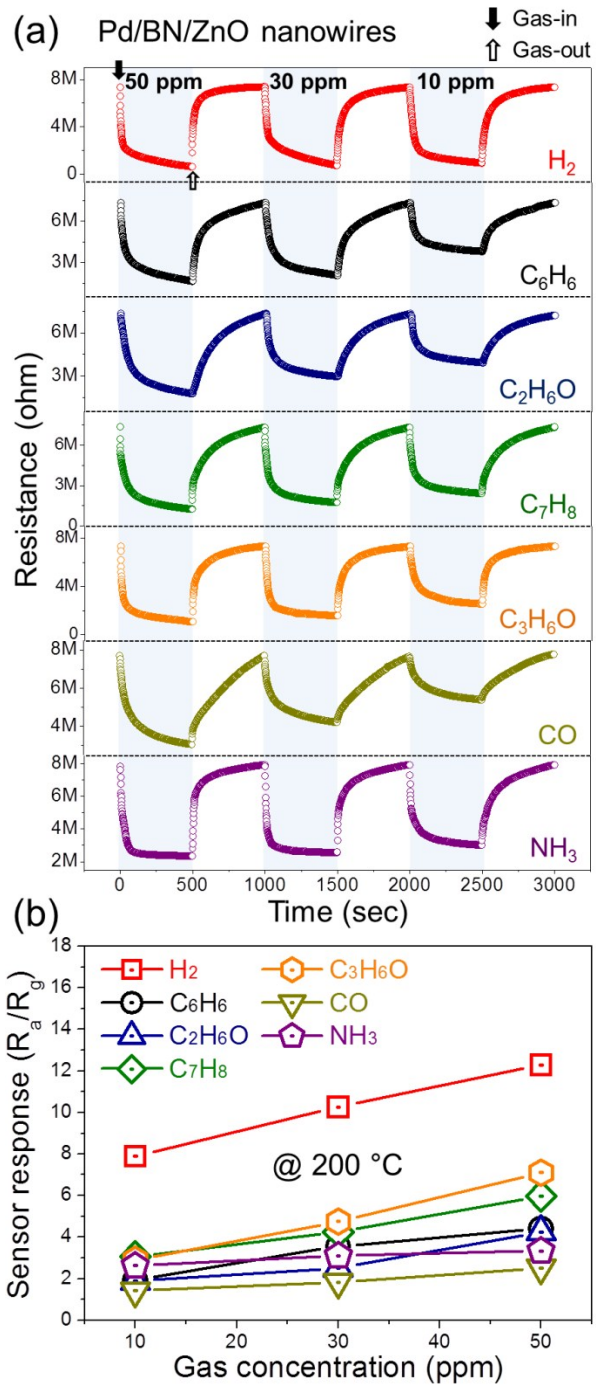

Figure S11. (a) Dynamic resistance curves of Pd/BN/ZnO NWs towards 10, 30 and 50 ppm different gases at 200°C. (b) Corresponding calibration curve.

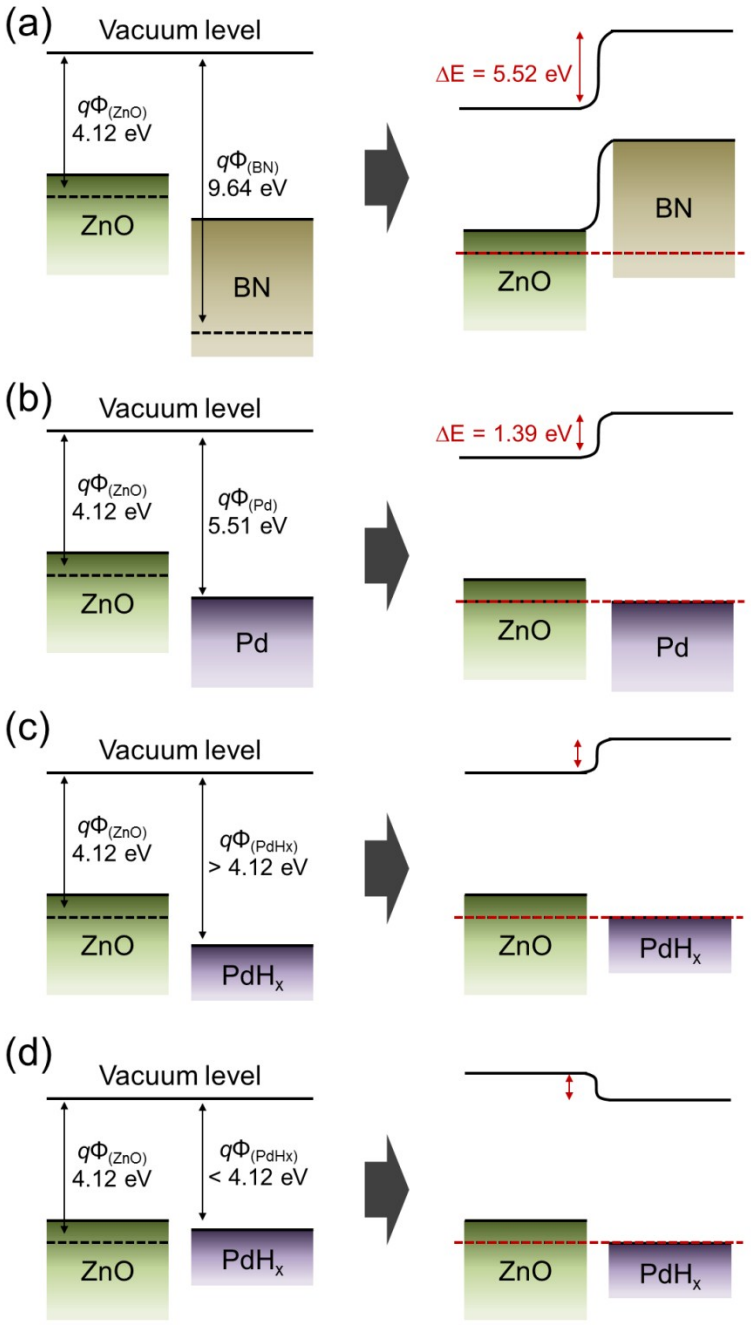

Figure S12. Energy levels of BN/ZnO and Pd/ZnO systems and formation of heterojunction barriers. (a) BN/ZnO, (b-d) Conversion of Schottcky contact to Ohmic contact in Pd/ZnO system in air and H_2 gas atmosphere.